

Article

Palladium(II) and Platinum(II) Deprotonated Diaminocarbene Complexes Based on *N*-(2-Pyridyl)ureas with Oxadiazole Periphery

Kirill K. Geyl¹, Svetlana O. Baykova¹, Pavel A. Andoskin², Vladimir V. Sharoyko^{1,2} , Anastasiya A. Eliseeva¹ , Sergey V. Baykov^{1,*} , Konstantin N. Semenov^{1,2}  and Vadim P. Boyarskiy¹ 

¹ Institute of Chemistry, Saint Petersburg State University, 7/9 Universitetskaya Nab., 199034 Saint Petersburg, Russia

² Department of General and Bioorganic Chemistry, Pavlov First Saint Petersburg State Medical University, 6–8 L'va Tolstogo Str., 197022 Saint Petersburg, Russia

* Correspondence: s.baykov@spbu.ru

Abstract: Metal mediated coupling of isocyanides with substituted *N*-(pyridine-2-yl) ureas was first used to incorporate privileged biological motifs into platinum metal complexes. We synthesized two palladium(II) and two platinum(II) cyclometallated species with oxadiazole cores. The compounds were isolated in good yields (61–73%) and characterized by high-resolution mass spectrometry and ¹H, ¹³C, and ¹⁹⁵Pt NMR spectroscopies. The structures of three complexes were additionally elucidated by X-ray diffraction analysis. These complexes indeed showed cytotoxic activity. The species bearing the 1,3,4-oxadiazole moiety exhibit more potency than the ones with the 1,2,4-oxadiazole ring. Particularly, the cytotoxic effect of both 1,3,4-oxadiazole-based complexes towards T98G cells significantly exceeds the common antitumor metal-drug cisplatin.

Keywords: cyclometallated platinum metal complexes; *N*-(pyridine-2-yl) ureas; metal mediated coupling; isocyanides; cytotoxic activity



Citation: Geyl, K.K.; Baykova, S.O.; Andoskin, P.A.; Sharoyko, V.V.; Eliseeva, A.A.; Baykov, S.V.; Semenov, K.N.; Boyarskiy, V.P. Palladium(II) and Platinum(II) Deprotonated Diaminocarbene Complexes Based on *N*-(2-Pyridyl)ureas with Oxadiazole Periphery. *Inorganics* **2022**, *10*, 247. <https://doi.org/10.3390/inorganics10120247>

Academic Editor: Hristo P. Varbanov

Received: 13 November 2022

Accepted: 5 December 2022

Published: 7 December 2022

Publisher's Note: MDPI stays neutral with regard to jurisdictional claims in published maps and institutional affiliations.



Copyright: © 2022 by the authors. Licensee MDPI, Basel, Switzerland. This article is an open access article distributed under the terms and conditions of the Creative Commons Attribution (CC BY) license (<https://creativecommons.org/licenses/by/4.0/>).

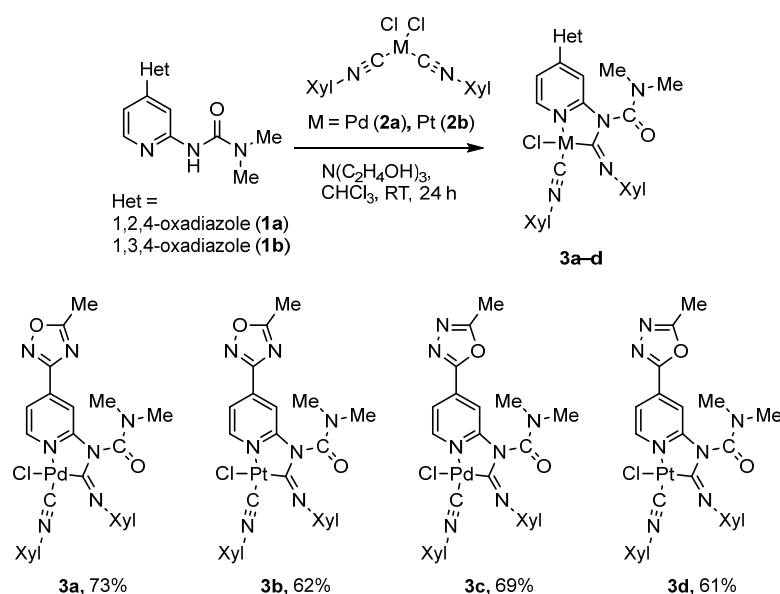
1. Introduction

Starting from the second half of the 20th century and up to the present, coordination compounds of platinum group metals with nitrogen-containing ligands have been widely used in the treatment of oncological diseases [1]. For many years, the recognized leader among such compounds was cisplatin, but, over time, its shortcomings began to appear more and more. Currently, one of the promising approaches for creating drugs with increased efficiency and a small number of side effects is the incorporation of various heterocyclic ligands into the structure of palladium(II) and platinum(II) complexes [2–5], as well as the use of cyclometallated species [3–5].

As a rule, the preparation of late transition metal complexes with cyclometallating (C^N) ligands includes a stage of a N^C–X bond selective intramolecular activation (X = H, halogen) [6]. Often, need for the activation narrows the range of possible products. Therefore, alternative methods for creating these metallacycles are of interest. One such method is the reaction of bis(isocyanide) metal complexes with poly-*N*-nucleophiles [7,8]. The products of this reaction are *C,N*-chelate deprotonated diaminocarbene species, which are actively used in various fields of chemistry [9]: catalysis of cross-coupling [10–15] and hydrosilylation [16–19], alkyne activation [20–22], and the sensing of mercury(II) ions in solution [23]. Chelate mono- and binuclear complexes of palladium(II) and platinum(II) that contain a diaminocarbene or aminoimidoyl (deprotonated diaminocarbene) fragment became convenient models for studying new types of noncovalent bonding in organometallic compounds [24]. In addition, these complexes have been shown to be promising luminescent materials [25] and antitumor cytotoxic agents [26,27].

In order for the preparation of cyclometallated platinum metal complexes based on coupling metal bis(isocyanide) species with poly-*N*-nucleophiles to make it possible to obtain a wide range of functionalized derivatives, availability of functionalized polynucleophiles is necessary. We have recently managed to solve this problem by developing a convenient method for the synthesis of pyridyl-substituted dialkylureas [28] and demonstrating their ability to act as polynucleophiles in the reaction with bis(isocyanide) complexes [17,29]. This opens the way for us to obtain cyclometallated complexes of platinum(II) and palladium(II) containing an additional heterocycle, for which we chose oxadiazoles in this work.

The reason for our choice was that both the 1,2,4-oxadiazole and 1,3,4-oxadiazole cores represent privileged motifs for anticancer research studies [30–38], including the design of antitumor metal agents [39]. Moreover, these heterocycles demonstrated acceptable pharmacokinetic profiles and low toxicity in many studies [40–43]. Therefore, in this work, we set ourselves the task of synthesizing *C,N*-cyclometallated platinum metal complexes functionalized with oxadiazole substituents (Scheme 1) and determining their antitumor activity.



Scheme 1. Synthesis of deprotonated diaminocarbene complexes with hybrid pyridylureas–oxadiazole ligands (3a–d).

2. Results and Discussion

2.1. Synthesis and Characterization of Complexes 3a–d

Recently we reported on synthesis of palladium(II) and platinum(II) deprotonated diaminocarbene complexes via the metal mediated nucleophilic addition of *N*-(pyridine-2-yl) ureas to isocyanides [17,18,29]. In these works, ureas bearing pyridine, picoline, quinoline, or isoquinoline moieties were only considered, whereas the reactivity of ureas with more complicated substituents such as heterocycles was not investigated. Notably, both 1,2,4- and 1,3,4-oxadiazole rings are able to coordinate to platinum metals [39,44,45] and hinder the aim reaction.

For the starting reaction conditions, we chose a previously used protocol: the treatment of equivalent amounts of oxadiazole substituted *N*-pyridylureas 1, *cis*-[MCl₂(CNXyl)₂] (M = Pd, 2a; Pt, 2b), and triethanolamine in CHCl₃ at RT for 24 h. However, the conversion of urea was not full in this reaction condition. So, the amounts of complex 2 and the base were increased up to 1.2 equiv, and, as a result, target chelate deprotonated diaminocarbene complexes 3a–d were obtained in moderate yields (61–73%) (Scheme 1).

All the synthesized compounds were characterized by NMR spectroscopy (^1H , ^{13}C , ^{195}Pt) and HR mass spectrometry. In NMR spectra (both ^1H and ^{13}C) of all these complexes, the splitting of methyl group signals in the NMe_2 moiety and in the xylyl ring of the diaminocarbene ligand was detected. According to our suggestion, this effect related to double-bond character of the carbon–nitrogen bond (C6–N3 in Table 1) and, therefore, the slower rotation around the C–N bond. The same effect was found for previously synthesized Pt(II) [17] and Pd(II) [29] deprotonated diaminocarbene complexes with coordinated *N*-pyridylureas. A broad doublet in the range of δ 9.29–9.48 ppm assigned to the α -CH proton of the pyridine ring was observed in all the ^1H NMR spectra. In uncoordinated ureas **1a** and **1b**, this proton gives signal at 8.31–8.45 ppm [46,47]. Such signal shifts are usual for azines coordinated by N atom to platinum metals [48,49], including other *N*-pyridylureas-based diaminocarbene complexes [17,18,29].

Table 1. Selected bond lengths and angles for complexes **3a–c** in the obtained solvates.

Parameter	3a ·1,2-DCE	3b ·1,2-DCE	3b ·1,2-DCEA	3c ·1 $\frac{1}{2}$ (1,2-DCE)	3c ·1 $\frac{1}{2}$ (1,2-DCE)A
M1–Cl1, Å	2.3912(5)	2.3895(13)	2.3821(12)	2.3856(11)	2.3866(11)
M1–N1, Å	2.0420(17)	2.036(4)	2.040(4)	2.053(4)	2.043(4)
M1–C6, Å	2.015(2)	2.005(5)	2.012(5)	2.006(4)	2.005(5)
Pd1–C15, Å	1.958(2)	1.928(5)	1.914(5)	1.954(4)	1.967(5)
C6–N2, Å	1.428(3)	1.441(6)	1.420(6)	1.421(5)	1.426(6)
C6–N3, Å	1.251(3)	1.261(7)	1.265(7)	1.259(6)	1.259(6)
C24–N2, Å	1.462(3)	1.461(6)	1.456(6)	1.465(5)	1.463(5)
C24–N5, Å	1.326(3)	1.338(7)	1.332(7)	1.327(6)	1.331(6)
C6–Pd1–N1, °	81.26(8)	81.48(18)	81.21(18)	81.76(16)	81.85(17)
N2–C6–N3, °	115.52(19)	113.6(4)	114.1(4)	115.3(4)	115.4(4)

M = Pd for **3a** and **3c**, Pt for **3b**.

The signals of ^{195}Pt are very similar (–3803 ppm for **3b** and –3802 ppm for **3d**) and close to relevant *N*-pyridylurea-based Pt(II) metallocycles (–3807––3809 ppm) [17,18]. In the HR-mass spectra of **3a–d**, $[\text{M–Cl}]^+$ ion peaks along with the characteristic isotopic distribution were observed.

Moreover, the thermal stability of synthesized complexes **3a–d** was characterized by thermogravimetric analysis (TGA). The TG/DTG curves are presented in Figures S6–S9 (Supplementary Materials). As demonstrated by the TGA results, these complexes have comparable thermal stability (up to 100–120 °C), regardless of the type of heterocyclic core or metal center.

2.2. Structural Studies

The structure of complexes **3a–c** (Figure 1; Figure S1, Supplementary Materials) in solid state was confirmed by X-ray diffraction (XRD) studies of corresponding solvates with 1,2-dichloroethane (**3a**·1,2-DCE, Figure S2; **3b**·1,2-DCE, Figure S3; **3c**·1 $\frac{1}{2}$ (1,2-DCE), Figure S4, Supplementary Materials). Details of the structure's solution and refinement are collected in Table S1 of Supplementary Materials. Values of bond lengths and angles are presented in Table 1. Since solvates **3b**·1,2-DCE and **3c**·1 $\frac{1}{2}$ (1,2-DCE) contain two crystallographically independent molecules of complexes, geometrical parameters of the environment of the metal center are given for both of them.

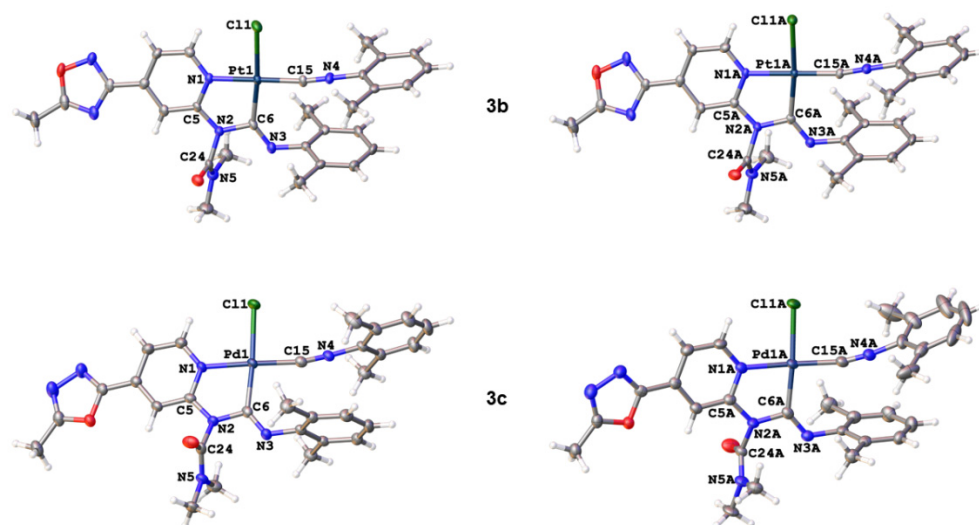


Figure 1. XRD structures of complexes **3b** and **3c**.

Crystals based on the complexes bearing 1,2,4-oxadiazole moiety (**3a**·1,2-DCE and **3b**·1,2-DCE) have the $P\bar{1}$ space group; whereas, in the 1,3,4-oxadiazole derivative (**3c**·1 $\frac{1}{2}$ 1,2-DCE), the $P2_1/n$ space group is realized. In general, the new complexes have the same structure as previously described: deprotonated diaminocarbene complexes with *N*-pyridylurea ligands [17,29]. In all cases, the metal is surrounded by three ligands: a bidentate amidine-like deprotonated diaminocarbene bearing the pyridine ring, an isocyanide, and a chloride anion, that forms slightly distorted square planar geometry.

A main packing feature of the new complexes in comparison to the early described ones [17,29] is $\pi\cdots\pi$ interactions between oxadiazole and pyridine moieties, similar to those studied in our recent work [47] (Figures 2 and S5). The crystal structures of (**3a,b**)·1,2-DCE and **3c**·1 $\frac{1}{2}$ 1,2-DCE exhibit 3D networks comprising the complexes and molecules of 1,2-dichloroethane, which are linked to each other via intermolecular C–H \cdots X (X = Cl, O) hydrogen bonds (HBs; Figures S2–S4, Supplementary Materials). The complexes are associated to each other by C–H \cdots Cl HBs between chloride centers and H-atoms of the ligands. At the same time, the complexes form intramolecular C–H \cdots Cl HBs between chloride ligands and Hs of the pyridine moieties (Figures S2–S4).

2.3. Cytotoxicity Assay

Considering our prominent interest in the search for new anticancer metal drugs [26,50–52], we evaluated the activity of the obtained deprotonated diaminocarbene complexes against several tumor cell lines, namely, A549 (lung carcinoma), PANC-1 (pancreatic carcinoma), and T98G (glioblastoma) using MMT test [53]. The received values of the half maximal inhibitory concentration (IC₅₀) are presented in Table 2.

The analysis of cytotoxicity assay results revealed that the complexes bearing 1,3,4-oxadiazole moiety (**3c** and **3d**) exhibit more potency than the complexes with 1,2,4-oxadiazole ring (**3a** and **3b**). Particularly, the cytotoxic effect of both 1,3,4-oxadiazole-based complexes (**3c** and **3d**) toward T98G cells significantly exceeds the common antitumor metal-drug cisplatin (Table 2; 34.7–39.4 vs. 140 μ M). Moreover, palladium(II) derivative **3c** has shown slightly higher activity against PANC-1 cell line than the reference compound (10.3 vs. 16.44 μ M).

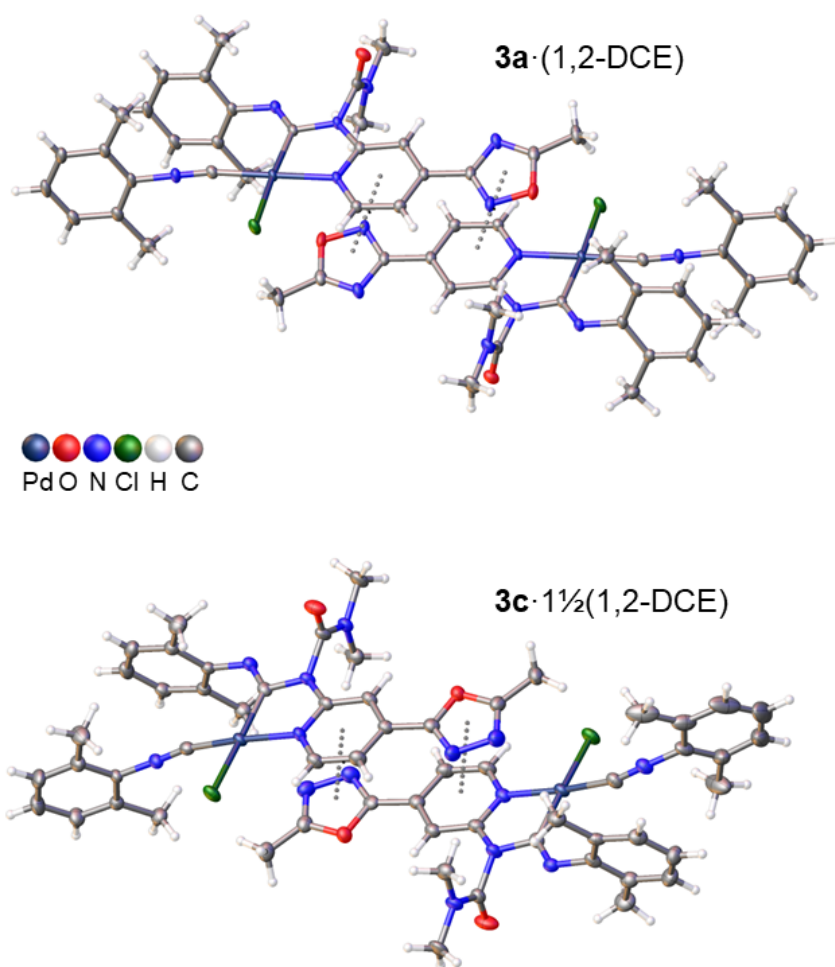


Figure 2. Oxadiazole–pyridine $\pi\cdots\pi$ interactions in the XRD structures of **3a**·(1,2-DCE) (*top*) and **3c**·1½(1,2-DCE) (*bottom*).

Table 2. The cytotoxic activity of complexes **3a–d** and cisplatin as reference compound determined by the MTT assay. The data presented were obtained from three independent experiments, and the values for IC₅₀ are mean \pm SD.

Compound	IC ₅₀ , μ M		
	A549	PANC-1	T98G
3a	98.0 \pm 9.8	85.1 \pm 8.5	>100
3b	64.6 \pm 6.0	95.0 \pm 9.5	100.0 \pm 10.0
3c	32.2 \pm 3.0	10.3 \pm 1.5	34.7 \pm 3.5
3d	47.1 \pm 5.0	40.6 \pm 4.6	39.4 \pm 3.9
Cisplatin	4.97 \pm 0.32 [54]	16.44 \pm 1.56 [55]	140 \pm 13 [56]

3. Materials and Methods

3.1. General

N-Oxides, [PdCl₂(MeCN)₂], K₂[PtCl₄], xylyl isocyanide, dimethyl cyanamide, methanesulfonic acid, and triethanolamine were obtained from commercial sources. Ureas **1a** [46] and **1b** [47], *cis*-[PdCl₂(CNXyl)₂] **2a** [57], and *cis*-[PtCl₂(CNXyl)₂] **2b** [58] were prepared according to previously reported procedures. All solvents were obtained from commercial sources and used without preliminary purification.

¹H, ¹³C, and ¹⁹⁵Pt NMR spectra were registered on a Bruker AVANCE III 400 spectrometer operating at room temperature (RT) at 400, 101, and 86 MHz for ¹H, ¹³C, and ¹⁹⁵Pt

NMR spectra, respectively. All spectra were recorded using CDCl_3 as a solvent. The chemical shifts are given in δ -values [ppm]. Multiplicities are abbreviated as follows: s = singlet, d = doublet, t = triplet, m = multiplet, br = broad; coupling constants, J , are reported in Hertz (Hz). High-resolution mass spectra (HRMS) were measured on Bruker Maxis HR-MS-ESI-qTOF using ESI. The most intense peak in the isotopic pattern is reported.

TGA was performed on ca. 4 mg samples of **3a–d** by using a Netzsch TG 209 F1 Libra thermal analyzer. The sample was dried under a vacuum at 50 °C before being heated from 40 to 450 °C at a heating rate of 10 K min^{-1} . A flow rate of 10 mL min^{-1} of dry argon was used to purge the sample.

3.2. Synthesis and Characterization of Complexes **3a–d**

Triethanolamine (0.12 mmol) was added to a mixture of the corresponding urea **1** (0.10 mmol) and *cis*- $[\text{MCl}_2(\text{CNXyl})_2]$ **2** (0.12 mmol) in CHCl_3 (3 mL). The reaction mixture was stirred at RT for 24 h. After that, the reaction mixture was filtered to remove a small amount of undissolved material (triethanolamine hydrochloride) and evaporated to dryness at 45 °C in vacuo. All obtained complexes were dissolved in dichloromethane (0.3 mL) and diluted with MeOH (1.5 mL). The formed precipitate was collected by filtration, washed with hexane, and dried in vacuo at RT.

Complex 3a. Light yellow powder; 73% yield (48 mg). ^1H NMR (400 MHz, CDCl_3): δ 9.29 (d, $J = 6.1$ Hz, 1H), 7.59 (d, $J = 6.2$ Hz, 1H), 7.53 (s, 1H), 7.16 (t, $J = 7.6$ Hz, 1H), 7.00 (d, $J = 7.7$ Hz, 2H), 6.82 (d, $J = 7.5$ Hz, 1H), 6.70 (d, $J = 7.5$ Hz, 1H), 6.24 (t, $J = 7.5$ Hz, 1H), 3.25 (s, 3H), 3.19 (s, 3H), 2.73 (s, 3H), 2.27 (s, 6H), 2.24 (s, 6H). ^{13}C NMR (101 MHz, CDCl_3): δ 177.79, 166.04, 158.16, 156.20, 153.50, 150.41, 148.86, 139.21, 134.30, 129.20, 128.93, 127.93, 127.59, 127.48, 127.36, 123.82, 113.25, 105.98, 38.36, 36.66, 19.71, 19.53, 18.50, 12.44. HRMS (ESI) m/z $[\text{M}-\text{Cl}]^+$ calculated for $[\text{C}_{29}\text{H}_{30}\text{ClN}_7\text{O}_2\text{Pd}-\text{Cl}]^+$ 614.1490; found 614.1527.

Complex 3b. Yellow powder; 62% yield (46 mg). ^1H NMR (400 MHz, CDCl_3): δ 9.45 (d, $J = 6.2$ Hz, 1H), 7.60 (dd, $J = 6.3, 1.7$ Hz, 1H), 7.57 (s, 1H), 7.15 (t, $J = 7.6$ Hz, 1H), 7.01 (d, $J = 7.6$ Hz, 2H), 6.79 (d, $J = 7.4$ Hz, 1H), 6.66 (d, $J = 7.5$ Hz, 1H), 6.17 (t, $J = 7.5$ Hz, 1H), 3.26 (s, 3H), 3.19 (s, 3H), 2.74 (s, 3H), 2.29 (s, 6H), 2.25 (d, $J = 3.3$ Hz, 6H). ^{13}C NMR (101 MHz, CDCl_3): δ 177.83, 166.00, 157.39, 153.75, 150.70, 148.99, 146.98, 139.30, 134.46, 128.97, 128.61, 127.91, 127.39, 127.31, 127.24, 123.25, 112.80, 106.06, 38.32, 36.67, 19.68, 19.43, 18.41, 12.43. ^{195}Pt NMR (86 MHz, CDCl_3): δ -3803.39. HRMS (ESI) m/z $[\text{M}-\text{Cl}]^+$ calculated for $[\text{C}_{29}\text{H}_{30}\text{ClN}_7\text{O}_2\text{Pt}-\text{Cl}]^+$ 703.2103; found 703.2140.

Complex 3c. Yellow powder; 69% yield (34 mg). ^1H NMR (400 MHz, CDCl_3): δ 9.34 (d, $J = 6.1$ Hz, 1H), 7.53 (dd, $J = 6.1, 1.6$ Hz, 1H), 7.51–7.47 (m, 1H), 7.17 (t, $J = 7.6$ Hz, 1H), 7.01 (d, $J = 7.7$ Hz, 2H), 6.83 (d, $J = 7.5$ Hz, 1H), 6.71 (d, $J = 7.5$ Hz, 1H), 6.26 (t, $J = 7.5$ Hz, 1H), 3.26 (s, 3H), 3.20 (s, 3H), 2.72 (s, 3H), 2.28 (s, 6H), 2.24 (s, 6H). ^{13}C NMR (101 MHz, CDCl_3): δ 165.38, 162.22, 158.00, 156.24, 153.39, 150.32, 149.23, 135.51, 134.29, 129.27, 128.86, 127.95, 127.55, 127.51, 127.39, 123.91, 112.18, 105.02, 38.42, 36.70, 19.72, 19.52, 18.49, 11.27. HRMS (ESI) m/z $[\text{M}-\text{Cl}]^+$ calculated for $[\text{C}_{29}\text{H}_{30}\text{ClN}_7\text{O}_2\text{Pd}-\text{Cl}]^+$ 614.1490; found 614.1476.

Complex 3d. Light yellow powder; 61% yield (45 mg). ^1H NMR (400 MHz, CDCl_3): δ 9.48 (d, $J = 6.3$ Hz, 1H), 7.54 (d, $J = 6.3$ Hz, 1H), 7.50 (s, 1H), 7.15 (t, $J = 7.6$ Hz, 1H), 7.01 (d, $J = 7.6$ Hz, 2H), 6.79 (d, $J = 7.4$ Hz, 1H), 6.66 (d, $J = 7.4$ Hz, 1H), 6.18 (t, $J = 7.5$ Hz, 1H), 3.26 (s, 3H), 3.19 (s, 3H), 2.71 (s, 3H), 2.28 (s, 6H), 2.24 (d, $J = 5.5$ Hz, 6H). ^{13}C NMR (101 MHz, CDCl_3): δ 165.45, 162.18, 157.41, 153.64, 150.59, 148.90, 147.36, 135.56, 134.45, 129.05, 128.52, 127.93, 127.42, 127.35, 127.19, 123.35, 111.77, 105.06, 38.38, 36.71, 19.69, 19.41, 18.40, 11.28. ^{195}Pt NMR (86 MHz, CDCl_3): δ -3802.34. HRMS (ESI) m/z $[\text{M}-\text{Cl}]^+$ calculated for $[\text{C}_{29}\text{H}_{30}\text{ClN}_7\text{O}_2\text{Pt}-\text{Cl}]^+$ 703.2103; found 703.2043.

3.3. Crystal Growth, Structure Solution and Refinement Details

All single crystalline samples were obtained via slow evaporation of 1,2-DCE solutions of corresponding complexes at room temperature. X-ray diffraction data were collected at a Rigaku XtaLAB Synergy-S (**3a**·1,2-DCE and **3b**·1,2-DCE) and at a Rigaku SuperNova (**3c**·1 $^{1/2}$ /1,2-DCE) diffractometers using Cu-K α ($\lambda = 0.154184$ nm) radiation.

The structures have been solved with the ShelXT [59] structure solution program using Intrinsic Phasing and refined with the ShelXL [60] refinement package incorporated in the OLEX2 program package [61] using Least Squares minimization. The carbon-bound H atoms were placed in calculated positions. Empirical absorption correction was applied in CrysAlisPro [62] program complex using spherical harmonics, implemented in SCALE3 ABSPACK scaling algorithm. Supplementary crystallographic data have been deposited at Cambridge Crystallographic Data Centre: 2217791 (**3a**·1,2-DCE), 2217807 (**3b**·1,2-DCE), and 2217808 (**3c**·1¹/2(1,2-DCE)). They can be obtained free of charge via www.ccdc.cam.ac.uk/data_request/cif (accessed on 13 November 2022).

3.4. Cytotoxicity Evaluation

The MTT-assay (colorimetric test using 3-(4,5-dimethylthiazol-2-yl)-2,5-diphenyl-tetrazolium bromide) was performed on human lung adenocarcinoma A549, human pancreatic adenocarcinoma PANC-1, and human glioblastoma T98G cell lines to measure the cytotoxicity of complexes **3a–d**. Dried powdered samples of complexes **3a–d** were dissolved in DMSO to obtain stock solutions, which were immediately used for the cytotoxicity evaluation.

A total of 5000 cells per well were seeded into a 96-well plate and incubated overnight in Dulbecco's Modified Eagle's culture Medium (DMEM) supplemented with 10% heat inactivated fetal calf serum (FCS) and penicillin-streptomycin (10 IU·mL⁻¹–100 µg·mL⁻¹). During this period, cells were attached to the surface of the wells. After this, fresh DMEM medium containing various concentrations of studied complexes **3a–d** was added to the wells, and the plate was placed in an incubator, 95% humidity, 20% O₂, 5% CO₂, 37 °C. After 48 h, 100 µL DMEM and 20 µL MTT-reagent (0.5 mg·mL⁻¹) were added to the wells and continued to incubate for 1 h. The supernatant was then removed, the formazan crystals formed during MTT recovery by viable cells were dissolved in DMSO, and the optical density was measured on a Allsheng AMR-100 microplate photometer (Hangzhou, China) at λ = 540 nm (subtracting background optical density at λ = 700 nm) [53].

The data presented were obtained from three independent experiments, and the values for IC₅₀ are mean ± SD.

4. Conclusions

Thus, we have shown that our proposed methodology for the synthesis of (C^N)-cyclometallated complexes of platinum metals by metal mediated coupling of isocyanides with substituted *N*-(pyridine-2-yl) ureas makes it easy to incorporate privileged biological heterocyclic motifs into metal complexes. In this work, we synthesized four cyclometallated complexes with oxadiazole cores. These complexes indeed showed cytotoxic activity. The complexes bearing 1,3,4-oxadiazole moiety exhibit more potency than the ones with 1,2,4-oxadiazole ring. Particularly, the cytotoxic effect of both 1,3,4-oxadiazole-based complexes (**3c** and **3d**) towards T98G cells significantly exceeds the common antitumor metal-drug cisplatin.

Supplementary Materials: The following are available online at <https://www.mdpi.com/article/10.3390/inorganics10120247/s1> and contains copies of NMR spectra for complexes **3a–d**, crystallographic information for crystals **3a**·1,2-DCE, **3b**·1,2-DCE, and **3c**·1¹/2(1,2-DCE) (Table S1), X-ray molecular structure of solvate **3a**·1,2-DCE (Figure S1), illustrations of hydrogen bonding in solvates **3a**·1,2-DCE (Figure S2), **3b**·1,2-DCE (Figure S3), **3c**·1¹/2(1,2-DCE) (Figure S4), illustration of oxadiazole-pyridine π···π interactions in the solvate **3b**·(1,2-DCE), as well as TGA curves (Figures S6–S9).

Author Contributions: Conceptualization, S.V.B.; methodology, S.V.B. and V.V.S.; investigation, K.K.G., S.O.B., P.A.A. and A.A.E.; writing—original draft preparation, S.V.B., V.V.S. and A.A.E.; writing—review and editing, K.N.S. and V.P.B.; visualization, A.A.E.; supervision, V.P.B. and K.N.S.; project administration, S.V.B. All authors have read and agreed to the published version of the manuscript.

Funding: The work was supported by the Russian Science Foundation (grant 22-73-10031; synthetic work, preparation of crystalline samples, and cytotoxicity evaluation) and the Council for Grants of the President of Russian Federation (grant MK-1614.2021.1.3; crystallographic studies).

Institutional Review Board Statement: Not applicable.

Informed Consent Statement: Not applicable.

Data Availability Statement: The data presented in this study are available on request from the corresponding author.

Acknowledgments: The authors are grateful to the Centre for Magnetic Resonance, Centre for X-ray Diffraction Studies, Centre for Chemical Analysis and Materials Research, Thermogravimetric and Calorimetric Research Centre (all belonging to Saint Petersburg State University) for physicochemical measurements.

Conflicts of Interest: The authors declare no competing interests.

Sample Availability: Samples of the compounds are not available from the authors.

References

1. Johnstone, T.C.; Suntharalingam, K.; Lippard, S.J. The Next Generation of Platinum Drugs: Targeted Pt(II) Agents, Nanoparticle Delivery, and Pt(IV) Prodrugs. *Chem. Rev.* **2016**, *116*, 3436–3486. [[CrossRef](#)] [[PubMed](#)]
2. Lazarević, T.; Rilak, A.; Bugarčić, Ž.D. Platinum, palladium, gold and ruthenium complexes as anticancer agents: Current clinical uses, cytotoxicity studies and future perspectives. *Eur. J. Med. Chem.* **2017**, *142*, 8–31. [[CrossRef](#)] [[PubMed](#)]
3. Czarnomysy, R.; Radomska, D.; Szewczyk, O.K.; Roszczenko, P.; Bielawski, K. Platinum and Palladium Complexes as Promising Sources for Antitumor Treatments. *Int. J. Mol. Sci.* **2021**, *22*, 8271. [[CrossRef](#)] [[PubMed](#)]
4. Alam, M.N.; Huq, F. Comprehensive review on tumour active palladium compounds and structure–activity relationships. *Coord. Chem. Rev.* **2016**, *316*, 36–67. [[CrossRef](#)]
5. Zou, T.; Lok, C.-N.; Wan, P.-K.; Zhang, Z.-F.; Fung, S.-K.; Che, C.-M. Anticancer metal-N-heterocyclic carbene complexes of gold, platinum and palladium. *Curr. Opin. Chem. Biol.* **2018**, *43*, 30–36. [[CrossRef](#)]
6. Dehand, J.; Pfeffer, M. Cyclometallated compounds. *Coord. Chem. Rev.* **1976**, *18*, 327–352. [[CrossRef](#)]
7. Boyarskiy, V.P.; Bokach, N.A.; Luzyanin, K.V.; Kukushkin, V.Y. Metal-mediated and metal-catalyzed reactions of isocyanides. *Chem. Rev.* **2015**, *115*, 2698–2779. [[CrossRef](#)]
8. Slaughter, L.M. “Covalent Self-Assembly” of Acyclic Diaminocarbene Ligands at Metal Centers. *Comments Inorg. Chem.* **2008**, *29*, 46–72. [[CrossRef](#)]
9. Kinzhalov, M.A.; Luzyanin, K.V. Reactivity of acyclic diaminocarbene ligands. *Coord. Chem. Rev.* **2019**, *399*, 213014. [[CrossRef](#)]
10. Singh, C.; Prakasham, A.P.; Gangwar, M.K.; Ghosh, P. Binuclear Fused 5-membered Palladacycle and Palladium Complex of Amido-Functionalized N-heterocyclic Carbene Precatalysts for the One-Pot Tandem Hiyama Alkynylation/Cyclization Reactions. *ChemistrySelect* **2018**, *3*, 9361–9367. [[CrossRef](#)]
11. Singh, C.; Prakasham, A.P.; Ghosh, P. Palladium Acyclic Diaminocarbene (ADC) Triflate Complexes as Effective Precatalysts for the Hiyama Alkynylation/Cyclization Reaction Yielding Benzofuran Compounds: Probing the Influence of the Triflate Co-Ligand in the One-Pot Tandem Reaction. *ChemistrySelect* **2019**, *4*, 329–336. [[CrossRef](#)]
12. Singh, C.; Prakasham, A.P.; Gangwar, M.K.; Butcher, R.J.; Ghosh, P. One-pot tandem hiyama alkynylation/cyclizations by palladium(II) acyclic diaminocarbene (ADC) complexes yielding biologically relevant benzofuran scaffolds. *ACS Omega* **2018**, *3*, 1740–1756. [[CrossRef](#)]
13. Boyarskiy, V.P.; Luzyanin, K.V.; Kukushkin, V.Y. Acyclic diaminocarbenes (ADCs) as a promising alternative to N-heterocyclic carbenes (NHCs) in transition metal catalyzed organic transformations. *Coord. Chem. Rev.* **2012**, *256*, 2029–2056. [[CrossRef](#)]
14. Mikhaylov, V.; Sorokoumov, V.; Liakhov, D.; Tskhovrebov, A.; Balova, I. Polystyrene-Supported Acyclic Diaminocarbene Palladium Complexes in Sonogashira Cross-Coupling: Stability vs. Catalytic Activity. *Catalysts* **2018**, *8*, 141. [[CrossRef](#)]
15. Mikhaylov, V.N.; Sorokoumov, V.N.; Korvinson, K.A.; Novikov, A.S.; Balova, I.A. Synthesis and Simple Immobilization of Palladium(II) Acyclic Diaminocarbene Complexes on Polystyrene Support as Efficient Catalysts for Sonogashira and Suzuki–Miyaura Cross-Coupling. *Organometallics* **2016**, *35*, 1684–1697. [[CrossRef](#)]
16. Gee, J.C.; Fuller, B.A.; Lockett, H.-M.; Sedghi, G.; Robertson, C.M.; Luzyanin, K.V. Visible light accelerated hydrosilylation of alkynes using platinum–[acyclic diaminocarbene] photocatalysts. *Chem. Commun.* **2018**, *54*, 9450–9453. [[CrossRef](#)]
17. Dobrynin, M.V.; Kasatkina, S.O.; Baykov, S.V.; Savko, P.Y.; Antonov, N.S.; Mikherdov, A.S.; Boyarskiy, V.P.; Islamova, R.M. Deprotonated diaminocarbene platinum complexes for thermoresponsive luminescent silicone materials: Both catalysts and luminophores. *Dalt. Trans.* **2021**, *50*, 14994–14999. [[CrossRef](#)]
18. Dobrynin, M.V.; Kasatkina, S.O.; Baykov, S.V.; Savko, P.Y.; Antonov, N.S.; Mikherdov, A.S.; Boyarskiy, V.P.; Islamova, R.M. Cyclometallated Platinum(II) Complexes for Obtaining Phenyl-Containing Silicone Rubbers via Catalytic Hydrosilylation Reaction. *Russ. J. Gen. Chem.* **2022**, *92*, 79–84. [[CrossRef](#)]

19. Chay, R.S.; Rocha, B.G.M.; Pombeiro, A.J.L.; Kukushkin, V.Y.; Luzyanin, K.V. Platinum Complexes with Chelating Acyclic Aminocarbene Ligands Work as Catalysts for Hydrosilylation of Alkynes. *ACS Omega* **2018**, *3*, 863–871. [[CrossRef](#)]
20. Barbazanges, M.; Fensterbank, L. Chiral Acyclic Diaminocarbene Complexes: A New Opportunity for Gold Asymmetric Catalysis. *ChemCatChem* **2012**, *4*, 1065–1066. [[CrossRef](#)]
21. Handa, S.; Slaughter, L.M. Enantioselective Alkynylbenzaldehyde Cyclizations Catalyzed by Chiral Gold(I) Acyclic Diaminocarbene Complexes Containing Weak Au-Arene Interactions. *Angew. Chem. Int. Ed.* **2012**, *51*, 2912–2915. [[CrossRef](#)] [[PubMed](#)]
22. Ruch, A.A.; Ellison, M.C.; Nguyen, J.K.; Kong, F.; Handa, S.; Nesterov, V.N.; Slaughter, L.M. Highly Sterically Encumbered Gold Acyclic Diaminocarbene Complexes: Overriding Electronic Control in Regiodivergent Gold Catalysis. *Organometallics* **2021**, *40*, 1416–1433. [[CrossRef](#)]
23. Eremina, A.A.; Kinzhalov, M.A.; Katlenok, E.A.; Smirnov, A.S.; Andrusenko, E.V.; Pidko, E.A.; Suslonov, V.V.; Luzyanin, K.V. Phosphorescent Iridium(III) Complexes with Acyclic Diaminocarbene Ligands as Chemosensors for Mercury. *Inorg. Chem.* **2020**, *59*, 2209–2222. [[CrossRef](#)] [[PubMed](#)]
24. Mikherdov, A.S.; Kinzhalov, M.A.; Novikov, A.S.; Boyarskiy, V.P.; Boyarskaya, I.A.; Dar'in, D.V.; Starova, G.L.; Kukushkin, V.Y. Difference in Energy between Two Distinct Types of Chalcogen Bonds Drives Regioisomerization of Binuclear (Diaminocarbene)Pd II Complexes. *J. Am. Chem. Soc.* **2016**, *138*, 14129–14137. [[CrossRef](#)] [[PubMed](#)]
25. Kinzhalov, M.A.; Grachova, E.V.; Luzyanin, K.V. Tuning the luminescence of transition metal complexes with acyclic diaminocarbene ligands. *Inorg. Chem. Front.* **2022**, *9*, 417–439. [[CrossRef](#)]
26. Serebryanskaya, T.V.; Kinzhalov, M.A.; Bakulev, V.; Alekseev, G.; Andreeva, A.; Gushchin, P.V.; Protas, A.V.; Smirnov, A.S.; Panikorovskii, T.L.; Lippmann, P.; et al. Water soluble palladium(II) and platinum(II) acyclic diaminocarbene complexes: Solution behavior, DNA binding, and antiproliferative activity. *New J. Chem.* **2020**, *44*, 5762–5773. [[CrossRef](#)]
27. Martínez-Junquera, M.; Lalinde, E.; Moreno, M.T.; Alfaro-Arnedo, E.; López, I.P.; Larráyo, I.M.; Pichel, J.G. Luminescent cyclometalated platinum(II) complexes with acyclic diaminocarbene ligands: Structural, photophysical and biological properties. *Dalt. Trans.* **2021**, *50*, 4539–4554. [[CrossRef](#)]
28. Rassadin, V.A.; Zimin, D.P.; Raskil'dina, G.Z.; Ivanov, A.Y.; Boyarskiy, V.P.; Zlotskii, S.S.; Kukushkin, V.Y. Solvent- and halide-free synthesis of pyridine-2-yl substituted ureas through facile C–H functionalization of pyridine N-oxides. *Green Chem.* **2016**, *18*, 6630–6636. [[CrossRef](#)]
29. Geyl, K.K.; Baykov, S.V.; Kasatkina, S.O.; Savko, P.Y.; Boyarskiy, V.P. Reaction of coordinated isocyanides with substituted N-(2-pyridyl)ureas as a route to new cyclometallated Pd(II) complexes. *J. Organomet. Chem.* **2022**, *980–981*, 122518. [[CrossRef](#)]
30. Krasavin, M.; Shetnev, A.; Sharonova, T.; Baykov, S.; Kalinin, S.; Nocentini, A.; Sharoyko, V.; Poli, G.; Tuccinardi, T.; Presnukhina, S.; et al. Continued exploration of 1,2,4-oxadiazole periphery for carbonic anhydrase-targeting primary arene sulfonamides: Discovery of subnanomolar inhibitors of membrane-bound hCA IX isoform that selectively kill cancer cells in hypoxic environment. *Eur. J. Med. Chem.* **2019**, *164*, 92–105. [[CrossRef](#)]
31. Shetnev, A.; Baykov, S.; Kalinin, S.; Belova, A.; Sharoyko, V.; Rozhkov, A.; Zelenkov, L.; Tarasenko, M.; Sadykov, E.; Korsakov, M.; et al. 1,2,4-Oxadiazole/2-Imidazoline Hybrids: Multi-target-directed Compounds for the Treatment of Infectious Diseases and Cancer. *Int. J. Mol. Sci.* **2019**, *20*, 1699. [[CrossRef](#)]
32. Glomb, T.; Szymankiewicz, K.; Świątek, P. Anti-Cancer Activity of Derivatives of 1,3,4-Oxadiazole. *Molecules* **2018**, *23*, 3361. [[CrossRef](#)]
33. Benassi, A.; Doria, F.; Pirota, V. Groundbreaking Anticancer Activity of Highly Diversified Oxadiazole Scaffolds. *Int. J. Mol. Sci.* **2020**, *21*, 8692. [[CrossRef](#)]
34. Kapoor, G.; Bhutani, R.; Pathak, D.P.; Chauhan, G.; Kant, R.; Grover, P.; Nagarajan, K.; Siddiqui, S.A. Current Advancement in the Oxadiazole-Based Scaffolds as Anticancer Agents. *Polycycl. Aromat. Compd.* **2022**, *42*, 4183–4215. [[CrossRef](#)]
35. Khan, I.; Ibrar, A.; Abbas, N. Oxadiazoles as Privileged Motifs for Promising Anticancer Leads: Recent Advances and Future Prospects. *Arch. Pharm.* **2014**, *347*, 1–20. [[CrossRef](#)]
36. Akhtar, J.; Khan, A.A.; Ali, Z.; Haider, R.; Shahar Yar, M. Structure-activity relationship (SAR) study and design strategies of nitrogen-containing heterocyclic moieties for their anticancer activities. *Eur. J. Med. Chem.* **2017**, *125*, 143–189. [[CrossRef](#)]
37. Desai, N.; Monapara, J.; Jethawa, A.; Khedkar, V.; Shingate, B. Oxadiazole: A highly versatile scaffold in drug discovery. *Arch. Pharm.* **2022**, *355*, 2200123. [[CrossRef](#)]
38. Bajaj, S.; Asati, V.; Singh, J.; Roy, P.P. 1,3,4-Oxadiazoles: An emerging scaffold to target growth factors, enzymes and kinases as anticancer agents. *Eur. J. Med. Chem.* **2015**, *97*, 124–141. [[CrossRef](#)]
39. Salassa, G.; Terenzi, A. Metal Complexes of Oxadiazole Ligands: An Overview. *Int. J. Mol. Sci.* **2019**, *20*, 3483. [[CrossRef](#)]
40. Boström, J.; Hogner, A.; Llinàs, A.; Wellner, E.; Plowright, A.T. Oxadiazoles in Medicinal Chemistry. *J. Med. Chem.* **2012**, *55*, 1817–1830. [[CrossRef](#)]
41. Flipo, M.; Desroses, M.; Lecat-Guillet, N.; Villemagne, B.; Blondiaux, N.; Leroux, F.; Piveteau, C.; Mathys, V.; Flament, M.-P.; Siepmann, J.; et al. Ethionamide Boosters. 2. Combining Bioisosteric Replacement and Structure-Based Drug Design to Solve Pharmacokinetic Issues in a Series of Potent 1,2,4-Oxadiazole EthR Inhibitors. *J. Med. Chem.* **2012**, *55*, 68–83. [[CrossRef](#)] [[PubMed](#)]
42. Boudreau, M.A.; Ding, D.; Meisel, J.E.; Janardhanan, J.; Spink, E.; Peng, Z.; Qian, Y.; Yamaguchi, T.; Testero, S.A.; O'Daniel, P.I.; et al. Structure–Activity Relationship for the Oxadiazole Class of Antibacterials. *ACS Med. Chem. Lett.* **2020**, *11*, 322–326. [[CrossRef](#)] [[PubMed](#)]

43. Ritchie, T.J.; Macdonald, S.J.F.; Peace, S.; Pickett, S.D.; Luscombe, C.N. The developability of heteroaromatic and heteroaliphatic rings—do some have a better pedigree as potential drug molecules than others? *Medchemcomm* **2012**, *3*, 1062. [[CrossRef](#)]
44. Bokach, N.A.; Khripoun, A.V.; Kukushkin, V.Y.; Haukka, M.; Pombeiro, A.J.L. A Route to 1,2,4-Oxadiazoles and Their Complexes via Platinum-Mediated 1,3-Dipolar Cycloaddition of Nitrile Oxides to Organonitriles. *Inorg. Chem.* **2003**, *42*, 896–903. [[CrossRef](#)] [[PubMed](#)]
45. Bokach, N.A.; Kukushkin, V.Y.; Haukka, M.; Pombeiro, A.J.L. Synthesis of (1,2,4-Oxadiazole)palladium(II) Complexes by [2 + 3] Cycloaddition of Nitrile Oxides to Organonitriles in the Presence of PdCl₂. *Eur. J. Inorg. Chem.* **2005**, *2005*, 845–853. [[CrossRef](#)]
46. Geyl, K.; Baykov, S.; Tarasenko, M.; Zelenkov, L.E.; Matveevskaya, V.; Boyarskiy, V.P. Convenient entry to N-pyridinylureas with pharmaceutically privileged oxadiazole substituents via the acid-catalyzed C H activation of N-oxides. *Tetrahedron. Lett.* **2019**, *60*, 151108. [[CrossRef](#)]
47. Baykov, S.; Mikherdov, A.; Novikov, A.; Geyl, K.; Tarasenko, M.; Gureev, M.; Boyarskiy, V. π - π Noncovalent Interaction Involving 1,2,4- and 1,3,4-Oxadiazole Systems: The Combined Experimental, Theoretical, and Database Study. *Molecules* **2021**, *26*, 5672. [[CrossRef](#)]
48. Bossi, A.; Rausch, A.F.; Leidl, M.J.; Czerwiec, R.; Whited, M.T.; Djurovich, P.I.; Yersin, H.; Thompson, M.E. Photophysical Properties of Cyclometalated Pt(II) Complexes: Counterintuitive Blue Shift in Emission with an Expanded Ligand π System. *Inorg. Chem.* **2013**, *52*, 12403–12415. [[CrossRef](#)]
49. Chassot, L.; Von Zelewsky, A. Cyclometalated complexes of platinum(II): Homoleptic compounds with aromatic C,N ligands. *Inorg. Chem.* **1987**, *26*, 2814–2818. [[CrossRef](#)]
50. Geyl, K.K.; Baykov, S.V.; Kalinin, S.A.; Bunev, A.S.; Troshina, M.A.; Sharonova, T.V.; Skripkin, M.Y.; Kasatkina, S.O.; Presnukhina, S.I.; Shetnev, A.A.; et al. Synthesis, Structure, and Antiproliferative Action of 2-Pyridyl Urea-Based Cu(II) Complexes. *Biomedicines* **2022**, *10*, 461. [[CrossRef](#)]
51. Matveevskaya, V.V.; Pavlov, D.I.; Sukhikh, T.S.; Gushchin, A.L.; Ivanov, A.Y.; Tennikova, T.B.; Sharoyko, V.V.; Baykov, S.V.; Benassi, E.; Potapov, A.S. Arene–Ruthenium(II) Complexes Containing 11H-Indeno [1,2-b]quinoxalin-11-one Derivatives and Tryptanthrin-6-oxime: Synthesis, Characterization, Cytotoxicity, and Catalytic Transfer Hydrogenation of Aryl Ketones. *ACS Omega* **2020**, *5*, 11167–11179. [[CrossRef](#)]
52. Boyarskii, V.P.; Mikherdov, A.S.; Baikov, S.V.; Savko, P.Y.; Suezov, R.V.; Trifonov, R.E. Diaminocarbene Complexes of Palladium(II) Containing 2-Aminooxazole and 2-Aminothiazole Heterocyclic Ligands as Potential Antitumor Agents. *Pharm. Chem. J.* **2021**, *55*, 130–132. [[CrossRef](#)]
53. Mosmann, T. Rapid colorimetric assay for cellular growth and survival: Application to proliferation and cytotoxicity assays. *J. Immunol. Methods* **1983**, *65*, 55–63. [[CrossRef](#)]
54. Dai, C.-H.; Li, J.; Chen, P.; Jiang, H.-G.; Wu, M.; Chen, Y.-C. RNA interferences targeting the Fanconi anemia/BRCA pathway upstream genes reverse cisplatin resistance in drug-resistant lung cancer cells. *J. Biomed. Sci.* **2015**, *22*, 77. [[CrossRef](#)]
55. Savić, A.; Gligorijević, N.; Arandjelović, S.; Dojčinović, B.; Kaczmarek, A.M.; Radulović, S.; Van Deun, R.; Van Hecke, K. Antitumor activity of organoruthenium complexes with chelate aromatic ligands, derived from 1,10-phenanthroline: Synthesis and biological activity. *J. Inorg. Biochem.* **2020**, *202*, 110869. [[CrossRef](#)]
56. Potapova, O.; Haghghi, A.; Bost, F.; Liu, C.; Birrer, M.J.; Gjerset, R.; Mercola, D. The Jun Kinase/Stress-activated Protein Kinase Pathway Functions to Regulate DNA Repair and Inhibition of the Pathway Sensitizes Tumor Cells to Cisplatin. *J. Biol. Chem.* **1997**, *272*, 14041–14044. [[CrossRef](#)]
57. Mikherdov, A.S.; Orekhova, Y.A.; Boyarskii, V.P. Formation of Homo- and Heteronuclear Platinum(II) and Palladium(II) Carbene Complexes in the Reactions of Coordinated Isocyanides with Aminothiazaheterocycles. *Russ. J. Gen. Chem.* **2018**, *88*, 2119–2124. [[CrossRef](#)]
58. Luzyanin, K.V.; Pombeiro, A.J.L.; Haukka, M.; Kukushkin, V.Y. Coupling between 3-Iminoisindolin-1-ones and Complexed Isonitriles as a Metal-Mediated Route to a Novel Type of Palladium and Platinum Iminocarbene Species. *Organometallics* **2008**, *27*, 5379–5389. [[CrossRef](#)]
59. Sheldrick, G.M. SHELXT—Integrated space-group and crystal-structure determination. *Acta Crystallogr. Sect. A Found. Adv.* **2015**, *71*, 3–8. [[CrossRef](#)]
60. Sheldrick, G.M. Crystal structure refinement with SHELXL. *Acta Crystallogr. Sect. C Struct. Chem.* **2015**, *71*, 3–8. [[CrossRef](#)]
61. Dolomanov, O.V.; Bourhis, L.J.; Gildea, R.J.; Howard, J.A.K.; Puschmann, H. OLEX2: A complete structure solution, refinement and analysis program. *J. Appl. Crystallogr.* **2009**, *42*, 339–341. [[CrossRef](#)]
62. CrysAlis Pro. *Data Collection and Processing Software for Agilent X-ray Diffractometers*; Agilent Technologies: Yarnton, UK, 2013.